

Supramolecular vs Electronic Structure: The Effect of the Tilt Angle of the Active Group in the Performance of a Molecular Diode

Peng Song,[†] Li Yuan,[†] Max Roemer,[†] Li Jiang,[†] and Christian A. Nijhuis^{*,†,‡}

[†]Department of Chemistry, National University of Singapore, 3 Science Drive 3, Singapore, 117543

[‡]Centre for Advanced 2D Materials and Graphene Research Centre, National University of Singapore, 6 Science Drive 2, Singapore, 117546

S Supporting Information

ABSTRACT: It is important to understand how the supramolecular structure of molecular junctions affects their performance. Such studies are challenging because it is difficult to separate electronic effects from supramolecular structural effects because both depend on each other. Here we show that by changing the connector group that connects the active component (a ferrocene unit) of a molecular diode to the backbone (an alkyl chain), both the electronic and supramolecular structures of the junctions are modified. The connector group determines the tilt angle of the Fc unit which in turn affects the packing structure of the molecular diodes. In this case, the supramolecular structure dominates over the electronic structure of the molecular diodes, and junctions with loosely packed SAMs result in poorly performing molecular diodes, while stiff, densely packed SAMs result in well-performing molecular diodes.

To develop molecular diodes has been one of the major goals in molecular electronics, but to date well-performing molecular diodes are still very rare. Ratner and Aviram theoretically proposed that molecular junctions could rectify currents in 1974.¹ They suggested that molecules of the form of donor-bridge-acceptor connected to two electrodes would result in metal-molecule-metal junctions that block the current in one direction of bias but would let the current pass through at opposite bias. Since then these² and other types of molecular diodes (e.g., based on only donor or acceptor groups asymmetrically positioned inside the junctions,³ push-pull molecules (strong dipoles),⁴ or molecules in an electrochemically controlled environment⁵ or asymmetrical metal-molecule contacts⁶) have been both experimentally and theoretically investigated. By far most studies have focused on how the chemical structure of the molecule would affect the electronic structure of the junctions, and the molecular diode performance was usually measured in terms of the rectification ratio R ($\equiv J(-V)/J(V)$). On paper, promising molecular diodes had often (apart from a few exceptions with high values of R)^{3a-c,5} disappointingly low values of $R < 10$ for unclear reasons. Therefore, it is important to identify, and isolate, potential factors that lower the performance of molecular diodes. Such studies, however, are challenging because molecular junctions are complex physicochemical systems making it difficult to isolate each factor that contributes to the charge transport character-

istics of the junctions. For the molecular diode shown in Figure 1, we have shown before that the surface roughness of the bottom electrode,⁷ purity of the monolayer precursors,⁸ the type of anchoring group,⁸ position of the ferrocene (Fc) unit within the SAM (i.e., length of the linker group),⁹ and the Fc-electrode interaction,⁹ all affect the diode performance. Here we show in general that the connector group X of the molecular precursor plays a critical role in the performance of our molecular diode and adds to the emerging conclusion that each component of the junctions have to be optimized to obtain well-performing diodes with $R > 100$.

Usually, the molecular component of the junctions is a complex chemical architecture consisting of several components as outlined in Figure 1a. The molecular structure contains at least four parts: (i) one or two anchoring groups to bind the molecule to one or both electrodes chemically (here only one anchoring group is drawn and such a molecule forms noncovalent SAM//top-contact); (ii) a linker group to bind the active component of the molecule to the anchoring group; (iii) the active component of the molecule (e.g., donor, acceptor, or a donor-bridge-acceptor moiety); and (iv) connector moieties (denoted as X) that connect the active component to the linker groups. Although the effects of different types of anchoring groups (e.g., thiolates, amines, or CN)^{6b,10} and linker groups (aliphatic, conjugated, or aromatic groups)^{3a,4b,5} on the diode performance have been studied systematically before, the connector moieties have been usually chosen for synthetic considerations, and their role in the performance of molecular diodes has not been systematically investigated.

We have studied a molecular diode based on a single electron donor asymmetrically positioned inside junctions of the form $\text{Ag}^{\text{TS}}\text{-SC}_n\text{Fc//GaO}_x/\text{EGaIn}$, where Ag^{TS} denotes template-stripped silver, SC_nFc denotes a SAM of $\text{S}(\text{CH}_2)_n\text{Fc}$ with Fc indicates ferrocene, and n denotes the number of CH_2 units (Figure 1b).^{3a} These junctions fabricated on Ag^{TS} have large enough values of R of 1.0×10^2 to be useful in physicochemical studies of charge transport.^{3a} We used Ag^{TS} surfaces as previous studies have shown that our diodes perform better on Ag^{TS} than on template-stripped gold (Au^{TS}) (by a factor of 10 in terms of R) because on Ag^{TS} the SAMs are less tilted and pack better than on Au^{TS} , and Ag^{TS} surfaces are smoother than Au^{TS} (rms is 0.68 nm for Au^{TS} and 0.30 nm for Ag^{TS} measured over $1.0 \times 1.0 \mu\text{m}^2$; Figure S1).⁷ Here, we used Ag^{TS} as the bottom electrode to

Received: February 29, 2016

Published: April 27, 2016

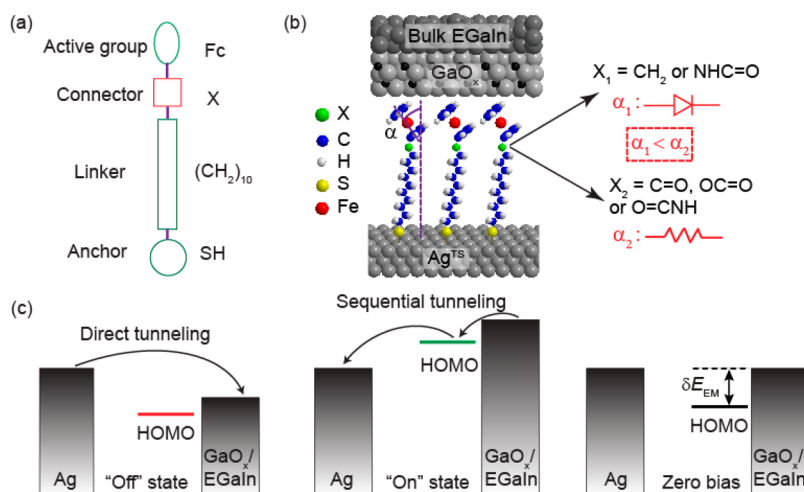


Figure 1. Schematic of the (a) molecular structure and (b) $\text{Ag}^{\text{TS}}\text{-SC}_{10}\text{XFc//GaO}_x\text{/EGaIn}$ junctions. Whether the junction behaves as a molecular diode or molecular resistor depends on α as explained in the main text. (c) Energy level diagram of the junctions in the “off” state at negative bias (left), “on” state at positive bias (middle), and at zero bias (right).

Table 1. Summary of the Characteristics of SAMs with Different X

X	E_{HOMO} (eV)		Γ_{Fc} (10^{-10} mol/cm 2)			ϕ^b (eV)	δE_{EM}^b (eV)	E_{LUMO}^b (eV)	thickness (Å)		α^e (°)	$R(\sigma_{\text{log}})$
	CV a,c	UPS b	CV a,c	XPS c	XPS d				CPK			
NHC=O	-4.95 ± 0.01	-5.00	4.58 ± 0.09	4.97	4.11	0.89	-2.51	18.9	16.7	47.9	90 (0.34)	
CH $_2$	-5.02 ± 0.01	-5.18	4.33 ± 0.08	4.50	3.95	1.23	-2.65	17.4	16.4	53.0	99 (0.39)	
O=C=O	-5.21 ± 0.01	-5.66	3.67 ± 0.28	4.04	4.24	1.42	-3.24	19.4	17.5	54.4	0.5 (0.15)	
O=CNH	-5.20 ± 0.01	-5.46	3.31 ± 0.13	3.41	4.09	1.37	-2.59	20.1	17.6	57.8	0.4 (0.43)	
C=O	-5.25 ± 0.01	-5.64	3.16 ± 0.10	2.57	4.47	1.17	-3.17	17.8	16.5	59.4	0.6 (0.30)	

a Error bars represent the standard deviation of three independent measurements. b Values were determined with an instrumental error of ± 0.05 eV. c Error is $\sim 2\%$ as estimated from the fits of the peak of Fe 2p spectra. d Values were determined with error of ± 2.0 Å, which represents the error of the fits. e Values were determined by NEXAFS with an instrumental error of $\pm 5^\circ$.

support a SAM of SC_{10}XFc , where X denotes the connector group with $X = \text{CH}_2$, $\text{C}=\text{O}$, $\text{O}-\text{C}=\text{O}$, $\text{NHC}=\text{O}$, or $\text{O}=\text{CNH}$. The well-characterized cone-shaped $\text{GaO}_x\text{/EGaIn}^{12}$ was used as top electrodes and completed the $\text{Ag}^{\text{TS}}\text{-SC}_{10}\text{XFc//GaO}_x\text{/EGaIn}$ junctions (Figure 1b). These junctions rectify due to a change in charge transport mechanism from sequential tunneling in the “on” state to direct tunneling in the “off” state (Figure 1c). 3c,9,13 Here we report that the connector moiety determines the tilt angle α of the Fc units (Figure 1b) which in turn directly relates to the supramolecular structure of the SAMs (i.e., the packing structure) and consequently to the performance of the molecular diodes in terms of R and leakage currents (the current in the “off” state; Figure 1c). We have shown before that in the specific case of $X = \text{CH}_2$, so-called odd–even effects are important: less densely packed SAMs with an even number of CH_2 units result in lower R (by a factor of 10) compared with densely packed SAMs with an odd number of CH_2 units 3a,11 because of an odd–even in α of 5° (for $n = 8-13$). Here we explicitly show by changing α over 11° that the connector group in general determines α and therefore plays a crucial role in the packing structure of SAMs directly affecting the performance of molecular diodes. Although we investigate both electron-donating and -withdrawing X moieties, we found that the changes in the supramolecular structure dominated over the changes in the electronic structure.

In general, it is challenging to disentangle how the electronic and supramolecular structures of the junctions contribute to the electrical characteristics of molecular junctions because one depends on the other. For this reason we characterized the

supramolecular and electronic structures of the SAMs in detail (the results are summarized in Table 1 and Figure 2, see SI for details). The SAMs on Au^{TS} were characterized with cyclic voltammetry (CV) to determine the surface coverage (Γ_{Fc}), peak anodic (E_{pa}), and cathodic (E_{pc}) potentials, and the energy level of the highest occupied molecular orbital (E_{HOMO}) which is centered at the Fc unit. A single reversible oxidation peak was observed for all SAMs suggesting that the SAMs were homogeneous (Figure 2a). 8,14 As expected, the value of E_{pa} shifted to more positive values when X is electron withdrawing ($X = \text{C}=\text{O}$, $\text{O}-\text{C}=\text{O}$, and $\text{O}=\text{CNH}$) and to more negative values when X is electron donating ($X = \text{NHC}=\text{O}$) relative to the E_{pa} value for SAMs with a weakly electron-donating group $X = \text{CH}_2$. These observations agree well with the observations made by others, 15 and here the E_{pa} shifted anodically over a range of 0.29 V in the order of $\text{C}=\text{O} > \text{O}-\text{C}=\text{O} > \text{O}=\text{CNH} > \text{CH}_2 > \text{NHC}=\text{O}$, which is consistent with the electronic effects (σ_{p} , sum of inductive (σ_{I}) and resonance (σ_{R}) components) 16 induced by different X (Table S1 and Figure S2).

The E_{HOMO} , the work function of the silver electrode ϕ_{Ag} , and the offset in energy between the E_{HOMO} and the Fermi-level of the bottom electrode δE_{EM} (Figure 1c) were determined by ultraviolet photoelectron spectroscopy (UPS, Figure S3). Table 1 and Figure 2b show that the general trend in the values of E_{HOMO} , determined by UPS and CV, agrees well, and the difference in absolute values is likely caused by the different experimental conditions. It is well-known that the ϕ_{Ag} decreases once a SAM is immobilized on Ag as result of the push-back effect that arises from the increase of density of states due to the

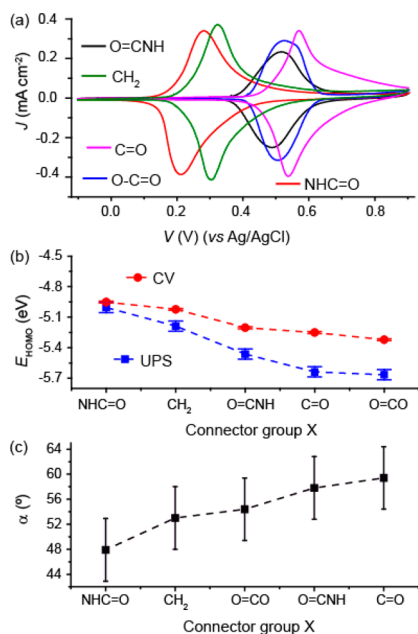


Figure 2. (a) Cyclic voltammograms (scan rate = 1.0 V/s) of the SAMs on Au^{TS} electrodes. (b) E_{HOMO} and (c) tilt angle α (as indicated in Figure 1) as a function of connector group X (see Table 1 for the meaning of the error bars).

formation of Ag–S bonds.¹⁷ For a clean Ag, $\phi_{\text{Ag}} = 4.7$ eV, and indeed, we found lower values of ϕ_{Ag} of 4.0–4.5 eV for the Ag^{TS}-SAM surfaces. The values of δE_{EM} range from 0.89 to 1.42 eV which are likely caused by the surface dipole induced by the dipole of X.¹⁸

We used near edge X-ray adsorption fine structure (NEXAFS) spectroscopy to determine α and the energy of the lowest unoccupied molecular orbital (E_{LUMO}).¹⁹ The tilt angle can be determined because of the linear dichroism in the X-ray absorption process. By recording the NEXAFS spectra at different angles θ , one can determine the tilt angle of specific moieties within the SAM (SI, page S11). We recorded the NEXAFS spectra at $\theta = 20^\circ$ and 90° (Figure S3) and used the change in the intensity of the C 1s $\rightarrow 4e_{1g}$ signal (285.4 eV) to determine α which are plotted in Figure 2c. Two SAMs with X = CH₂ and NHC=O have smaller values of α than the other three SAMs. These smaller α values indicate that the Fc units of these two SAMs are standing more upright than the other three. The E_{LUMO} is listed in Table 1, and we believe that the LUMO does not anticipate in charge transport in the applied bias range (see below) due to the large HOMO–LUMO gap. We used angle resolved X-ray photoemission spectroscopy (ARXPS) to further study the effects of the X on the supramolecular structures these SAMs on Ag^{TS}. Figures S4 and S5 show the Fe 2p and S 2p spectra of all SAMs from which we determined Γ_{Fc} and the effective thickness d of the SAMs using previously reported methods (SI, page S12). The surface coverages derived from XPS agree well with those derived from CV, and the values of d agree within the experimental error to the molecular lengths obtained by CPK models (Table 1).

The Ag^{TS}-SC₁₀XFc//GaO_x/EGaIn junctions were formed with cone-shaped GaO_x/EGaIn top electrodes, and charge transport properties were measured by recording the $J(V)$ curves ($0 \rightarrow +1.0 \text{ V} \rightarrow -1.0 \text{ V} \rightarrow 0$ in steps of 50 mV) using previously reported procedures (SI, page S12).^{3a} The $J(V)$ curves were recorded with average yield of 92% (Table S2). The large

number of $J(V)$ data were analyzed to determine the Gaussian mean of the values of $\log_{10}|J|$ ($\langle \log_{10}|J| \rangle_G$) for each measured bias. Figure S6 shows $\langle \log_{10}|J| \rangle_G$ vs applied bias curves, and the error bars indicate the log-standard deviation (σ_{\log}). Similarly, we determined the Gaussian mean of the values of $\log_{10}R$ ($\langle \log_{10}R \rangle_G$) and their log-standard deviations (see Table 1). Figure S7 shows the histograms of R for junctions with different X, and Figure 3a shows R vs X. The highest value of R of nearly 2

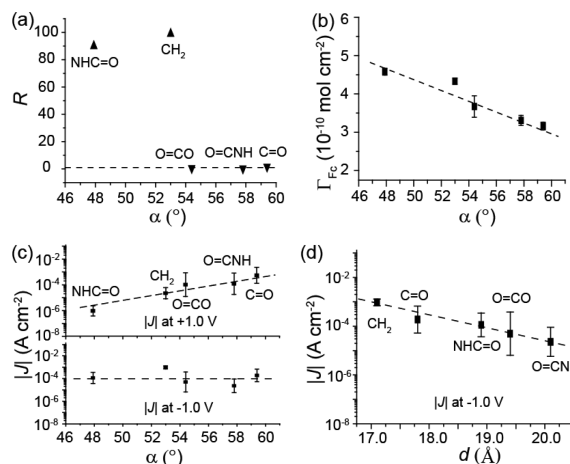


Figure 3. (a) Value of R as a function of α . The horizontal dashed line indicates $R = 1$. (b) Surface coverage of the SAMs as a function of α . (c) Current density at +1.0 V and -1.0 V as a function of α for junctions with different X. (d) Current density at -1.0 V as a function of d obtained from ARXPS. All the dashed lines are a guide for the eye.

orders of magnitude was observed for junctions with X = NHC=O and CH₂, while R was near unity for junctions with X = C=O, O–C=O, and O=CNH, and hence these junctions did not rectify significantly. The value of R for junctions with X = CH₂ is consistent with previous reports.^{3a,13} These data show that X plays a crucial role in the performance of the molecular diodes.

To elucidate that indeed the supramolecular structure of the SAM is determined by the tilt angle, we plotted Γ_{Fc} against α (Figure 3b). The good linear correlation indicates that the SAM structure relates directly to α which in turn is dictated by X. Figure 3c shows the correlation between α and values of J at +1.0 V. The leakage current increases by 2 orders of magnitude with increasing α of $\sim 11^\circ$ which confirms that the X is important to minimize leakage currents. This large increase of the leakage current with α caused the decrease in R and, in effect, changed the junction from a molecular diode to a molecular resistor. Figure 3c also shows that the values of $J(-1.0)$ (current density in the “on” state) are not directly correlated with the value of α . The variation of $J(-1.0)$ is mainly due to the variation of d (Table 1 and Figure 3d). These results show that the leakage current is more sensitive to the supramolecular structure of SAMs than d or the electronic structure of the SAMs. We have shown elsewhere that the interaction strength of the Fc with the electrode is important.⁹ In the present study we did not change the interaction of the Fc with the top electrode and kept the linker length constant at $n = 10$, and thus we did not change the coupling strength of the Fc with bottom electrode. In addition, low values of δE_{HOMO} ensure that the diodes would switch to the “on” state at low applied bias because the HOMO would fall in the bias window at relatively low applied bias increasing the value of R . The connector group X changed the values of E_{HOMO} by

nearly 0.3 eV (Table 1), but we did not observe a clear correlation between E_{HOMO} and R , which indicates that the effect of electronic structure is overshadowed by the supramolecular structure.

In summary, we studied how a connector group X that connects an electron donor to the backbone of the SAM influences the performance of a molecular diode of the form of $\text{Ag}^{\text{TS}}\text{-SC}_{10}\text{-XFc//GaO}_x\text{/EGaIn}$. These connector groups are often chosen based on synthetic grounds, but here we show that the connector group plays a crucial role in the supramolecular packing of the SAMs and determines the value of α . SAMs with small α values are densely packed and once incorporated in tunneling junctions form good molecular diodes with values of R of nearly 2 orders of magnitude. In contrast, SAMs with large α values are sterically hindered which prevents the SAMs from packing well and lowers the surface coverage and the effective thickness of the SAMs; these SAMs result in poorly rectifying diodes with R close to unity because they suffer from large leakage currents.

The connector group also affects the electronic structure (the E_{HOMO} changed by 0.3 eV), and in principle, junctions with low δE_{HOMO} values should have low turn-on values and perform well. This change in the electronic structure, however, was overshadowed by the changes in the supramolecular structure resulting in junctions that ceased to rectify. Although it is important to optimize the electronic structure of molecular junctions in general, this work shows that optimization of the supramolecular structure is at least of equal importance to ensure optimal performance of molecular electronic junctions and that connector groups have to be taken into consideration in the rational design of molecular diodes.

■ ASSOCIATED CONTENT

📄 Supporting Information

The Supporting Information is available free of charge on the ACS Publications website at DOI: 10.1021/jacs.6b02208.

Experimental details and data (PDF)

■ AUTHOR INFORMATION

Corresponding Author

*chmnc@nus.edu.sg

Notes

The authors declare no competing financial interest.

■ ACKNOWLEDGMENTS

The National Research Foundation (NRF) is kindly acknowledged for supporting this research under the CRP program (award no. NRF-CRP 8-2011-07). We also acknowledge the Minister of Education (MOE) for supporting this research under award no. MOE2015-T2-1-050. Prime Minister's Office, Singapore under its medium-sized center program is also acknowledged for supporting this research. P.S. thanks Harshini Venkata Annadata for helpful discussions about the electronic effects. Yu Xiaojiang is kindly acknowledged for assisting at the SINS beamline at SLS under NUS core support C-380-003-003-001.

■ REFERENCES

- (1) Aviram, A.; Ratner, M. A. *Chem. Phys. Lett.* **1974**, *29*, 277.
- (2) (a) Metzger, R. M. *Chem. Rev.* **2015**, *115*, 5056. (b) Honciuc, A.; Jaiswal, A.; Gong, A.; Ashworth, K.; Spangler, C. W.; Peterson, I. R.; Dalton, L. R.; Metzger, R. M. *J. Phys. Chem. B* **2005**, *109*, 857.

- (3) (a) Nerngchamngong, N.; Yuan, L.; Qi, D.-C.; Li, J.; Thompson, D.; Nijhuis, C. A. *Nat. Nanotechnol.* **2013**, *8*, 113. (b) Yoon, H. J.; Liao, K.-C.; Lockett, M. R.; Kwok, S. W.; Baghbazadeh, M.; Whitesides, G. M. *J. Am. Chem. Soc.* **2014**, *136*, 17155. (c) Yuan, L.; Breuer, R.; Jiang, L.; Schmittel, M.; Nijhuis, C. A. *Nano Lett.* **2015**, *15*, 5506. (d) Kornilovitch, P. E.; Bratkovsky, A. M.; Stanley Williams, R. *Phys. Rev. B: Condens. Matter Mater. Phys.* **2002**, *66*, 165436. (e) Liu, R.; Ke, S.-H.; Yang, W.; Baranger, H. U. *J. Chem. Phys.* **2006**, *124*, 024718. (f) Jeong, H.; Kim, D.; Wang, G.; Park, S.; Lee, H.; Cho, K.; Hwang, W.-T.; Yoon, M.-H.; Jang, Y. H.; Song, H.; Xiang, D.; Lee, T. *Adv. Funct. Mater.* **2014**, *24*, 2472. (g) Lenfant, S.; Krzeminski, C.; Delerue, C.; Allan, G.; Vuillaume, D. *Nano Lett.* **2003**, *3*, 741.
- (4) (a) Elbing, M.; Ochs, R.; Koentopp, M.; Fischer, M.; von Hänisch, C.; Weigend, F.; Evers, F.; Weber, H. B.; Mayor, M. *Proc. Natl. Acad. Sci. U. S. A.* **2005**, *102*, 8815. (b) Díez-Pérez, I.; Hihath, J.; Lee, Y.; Yu, L.; Adamska, L.; Kozhushner, M. A.; Oleynik, I. I.; Tao, N. *Nat. Chem.* **2009**, *1*, 635.
- (5) Capozzi, B.; Xia, J.; Adak, O.; Dell, E. J.; Liu, Z.-F.; Taylor, J. C.; Neaton, J. B.; Campos, L. M.; Venkataraman, L. *Nat. Nanotechnol.* **2015**, *10*, 522.
- (6) (a) Batra, A.; Darancet, P.; Chen, Q.; Meisner, J. S.; Widawsky, J. R.; Neaton, J. B.; Nuckolls, C.; Venkataraman, L. *Nano Lett.* **2013**, *13*, 6233. (b) Van Dyck, C.; Ratner, M. A. *Nano Lett.* **2015**, *15*, 1577.
- (7) Yuan, L.; Jiang, L.; Thompson, D.; Nijhuis, C. A. *J. Am. Chem. Soc.* **2014**, *136*, 6554.
- (8) Jiang, L.; Yuan, L.; Cao, L.; Nijhuis, C. A. *J. Am. Chem. Soc.* **2014**, *136*, 1982.
- (9) Yuan, L.; Nerngchamngong, N.; Cao, L.; Hamoudi, H.; del Barco, E.; Roemer, M.; Sriramula, R. K.; Thompson, D.; Nijhuis, C. A. *Nat. Commun.* **2015**, *6*, 6324.
- (10) (a) Kushmerick, J. G.; Whitaker, C. M.; Pollack, S. K.; Schull, T. L.; Shashidhar, R. *Nanotechnology* **2004**, *15*, S489. (b) Lee, Y.; Carsten, B.; Yu, L. *Langmuir* **2009**, *25*, 1495.
- (11) Yuan, L.; Thompson, D.; Cao, L.; Nerngchamngong, N.; Nijhuis, C. A. *J. Phys. Chem. C* **2015**, *119*, 17910.
- (12) (a) Chiechi, R. C.; Weiss, E. A.; Dickey, M. D.; Whitesides, G. M. *Angew. Chem., Int. Ed.* **2008**, *47*, 142. (b) Simeone, F. C.; Yoon, H. J.; Thuo, M. M.; Barber, J. R.; Smith, B. J. *J. Am. Chem. Soc.* **2013**, *135*, 18131. (c) Suchand Sangeeth, C. S.; Wan, A.; Nijhuis, C. A. *Nanoscale* **2015**, *7*, 12061.
- (13) Nijhuis, C. A.; Reus, W. F.; Barber, J. R.; Dickey, M. D.; Whitesides, G. M. *Nano Lett.* **2010**, *10*, 3611.
- (14) (a) Nerngchamngong, N.; Thompson, D.; Cao, L.; Yuan, L.; Jiang, L.; Roemer, M.; Nijhuis, C. A. *J. Phys. Chem. C* **2015**, *119*, 21978. (b) Lee, L. Y. S.; Sutherland, T. C.; Rucareanu, S.; Lennox, R. B. *Langmuir* **2006**, *22*, 4438.
- (15) Batterjee, S. M.; Marzouk, M. I.; Aazab, M. E.; El-Hashash, M. A. *Appl. Organomet. Chem.* **2003**, *17*, 291.
- (16) Hansch, C.; Leo, A.; Taft, R. W. *Chem. Rev.* **1991**, *91*, 165.
- (17) Ishii, H.; Sugiyama, K.; Ito, E.; Seki, K. *Adv. Mater.* **1999**, *11*, 605.
- (18) Cahen, D.; Kahn, A.; Umbach, E. *Mater. Today* **2005**, *8*, 32.
- (19) Ruehl, E.; Hitchcock, A. P. *J. Am. Chem. Soc.* **1989**, *111*, 5069.